

## **MICROSCOPICAL OBSERVATION OF MODE I CRACK PROPAGATION IN CONCRETE SUBJECTED TO FATIGUE**

A. Toumi, A. Bascoul, and A. Turatsinze,  
Laboratoire Matériaux et Durabilité des Constructions, INSA/UPS,  
France.

### **Abstract**

Fatigue tests were carried out on notched micro-concrete beams subjected to three point bending tests. Microscopic observations and crack length measurements were made by means of the replica technique associated with scanning electron microscopy (SEM). Observations of fatigue crack growth both on the surface and inside the specimens are presented and compared with previous investigations in static tests. A comparison is also presented between the observed crack lengths and the ones estimated by compliance method. Finally the kinetic of crack growth is discussed through the Paris's law.

Key words : Replica, SEM, Fatigue, Damage, Crack length, Paris law.

### **1 Introduction**

Even though some works have been devoted to concrete fatigue (Hsu. 1984, Hordijk. 1990, Bazant and Xu. 1991, Bazant and Schell. 1993), the study of the kinetic of crack growth is not very developed. Generally, in mode I, the crack length under cyclic loading is indirectly evaluated by means of the compliance calibration method and attempts are made at expressing this growth in terms of the well known Paris's law.

Based on microscopic observations, the present work, deals with the description of the mechanism of crack growth in concrete under cyclic loading in a first section. In a second section, the rate of the observed crack growth is discussed in terms of Paris's law.

## 2 Experimental program.

The specimens were made of ordinary micro-concrete, using Portland cement and crushed marble aggregates. The ratios of the mix components to cement by weight were as follows : Portland cement : 1 (557 kg/m<sup>3</sup>), water : 0.52, aggregates ( $d_{\max} = 3.15$  mm) : 2.62. Bending specimens were sawed from initial slabs (500×90×90 mm), which had been cured in water for three weeks. The notches were made by means of plates, 5 mm thick, placed at the middle of the mould; the tip of each plate was cut to a 30° angle. The final dimensions of the specimens are presented in Fig. 1.

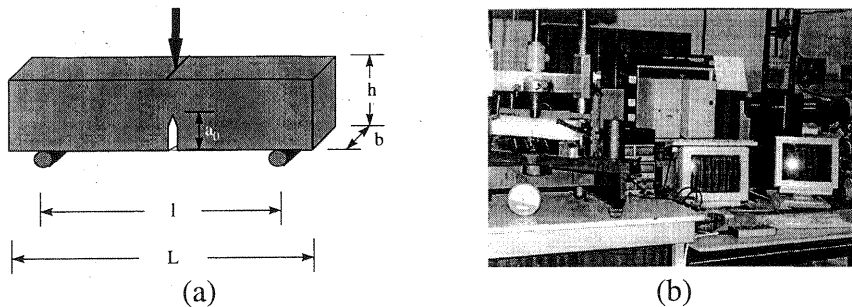


Fig. 1. (a) Specimen geometry; (b) Test arrangement and instrumentation

$$L = 420; l = 320; h = 80; b = 50; a_0 = 40 \quad (\text{mm})$$

Six cylinders of diameter 11,8 cm and 23,6 cm in height were also cast and tested at 28 days to determine the compressive strength and the Young's modulus. The compressive strength  $R_{c28}$  was  $56.9 \pm 4$  MPa and the average value of the secant Young's modulus was  $31600 + 2200$  MPa. The tensile strength  $R_{t28}$  estimated from BAEL formulas (BAEL91. 1992) was  $4.2 \pm 0.25$  MPa.

In order to minimise the crack propagation due to the hygrometric conditions, the fatigue tests were performed in a saturated atmosphere (100% HR, 23°C).

## 2.1 Loading equipment and instrumentation

All the tests were conducted in a closed loop digitally controlled machine, with a 45 kN load capacity. The crack mouth opening (CMOD) was measured by means of a LVDT located 10 mm below the notch. Data acquisition for both load and CMOD was performed by the computer controlling the test.

Microscopical observations were made by means of the replica technique in conjunction with scanning electron microscopy (SEM). For more information about this method, refer to Ollivier (1985). The resolution of the replication is about 0,1  $\mu\text{m}$ .

The replica method permits us to record the damage of concrete either on lateral surfaces of specimens or on sections of specimens. In the first case, it is a non destructive technique. Indeed, the evolution of the damage can be observed as a function of the load level in the case of the static tests or as a function of a number of cycles when the specimen is tested in fatigue. In the second case, it is a destructive technique, which makes possible the visualisation of the state of the damage inside the specimen for only one stage of loading.

## 2.2 Loading history

Prior to fatigue tests, 10 monotonic load controlled tests were performed to determine the average peak load  $P_u$  of the specimens. The measured peak loads are presented in table 1. These tests were also used to determine the load threshold beyond which a slow crack growth begins. They showed that a real micro-crack appears at about 60% of the mean peak load  $P_u$ . As our concern was to investigate the propagation of a real crack, the fatigue tests were conducted with different values of the upper load limit  $P_{\text{max}}$  beyond the characteristic load threshold equal to 0.98 - 0.97 - 0.93 - 0.94 - 0.87 - 0.81 - 0.76 and  $0.70P_u$ . The minimum load was approximately  $0,23P_u$  in all the tests. The frequency was 1 Hz.

Table 1. Static test results

Test number	1	2	3	4	5	6	7	8	9	10
Peak load (N)	980	840	840	920	820	760	840	920	920	900
Mean value (N)	864		Standard deviation %					7		

## 2.3 Preliminary fatigue tests

It is questionable whether the crack length "a" has the same value outside and inside a specimen. Indeed, under static tests the dye penetration technique (Bascoul et al. 1989) reveals a curvilinear shape of the crack

front through the specimen thickness. This is why the researchers use indirect methods such as compliance calibration to evaluate a mean crack length. In order to clarify this point, our program also included a lot of specimens which were subjected to fatigue tests for a different number of cycles and next sawed to compare the crack length inside and outside. As an example, the results for two specimens are presented in Fig. 2 in which we can observe a quasi linear shape of the crack front through the specimen thickness.

An additional work is presented here (Fig. 3) which compares crack lengths estimated by compliance calibration technique with actual crack lengths determined by the replica method. It can be seen from Fig. 3 that the compliance calibration technique underestimates the actual crack. Conversely, Swartz and Go (1984) showed that the compliance method overestimates the crack length obtained by the dye penetration.

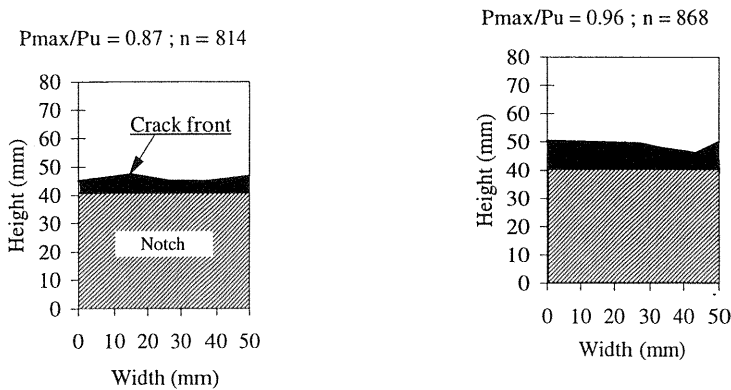


Fig. 2. Crack surfaces revealed by replica method

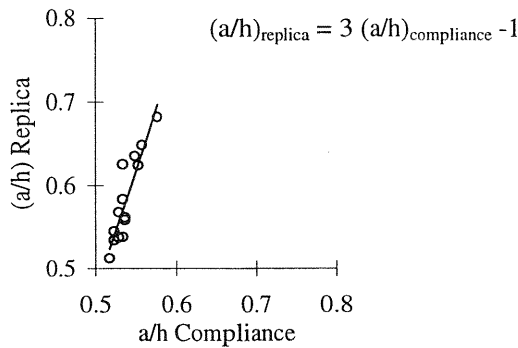


Fig. 3. Comparison of relative crack lengths obtained by replica technique to those obtained by compliance method for cracked specimens

### 3 Analysis of results

#### 3.1 Feature of crack growth

The feature of crack growth under static tests is similar in fatigue tests, but with some differences. Indeed, most of the investigations carried out on lateral surfaces, showed a complex crack growth process. For example, Fig. 4 gives the extracted crack path of one specimen which was subjected to 1500 cycles with  $0.85P_u$  as the upper load. Generally a unique crack propagates in the matrix and skirts round the aggregates along the well known interfacial transition zone (Fig. 4A). This mechanism which results in the deterioration of the bond between the coarse aggregate and the matrix is dominant, and is in agreement with the hypothesis formulated by Murdock and Kestler (1984) about the mechanism of fatigue crack growth in plain concrete. Sometimes, a crack runs across an aggregate as shown in Fig. 4B with a branching phenomenon within this aggregate. We must note that in this case, the observation of the initial state showed a pre-existing damage within the aggregate before the crack tip reached it. The crack is often composed of two branches (Fig. 4C). However only one of them is on the future main crack path. Due to the stress redistribution, the opening of other micro-cracks decreases but never closes completely and remains observable. When the crack stops in the matrix, two branches can be observed in the area of the crack end. When it stops in an aggregate as shown in Fig. 4D, there are no diffuse micro-cracks.

The observation of the crack propagation inside the material is similar to the one on the lateral surfaces. This point differs from static tests. Indeed, under static tests previous investigations (Bascoul and Turatsinze, 1994) showed discontinuous micro-cracks distributed ahead of the main path inside the specimens. This distribution is not observed in the case of fatigue tests. This phenomenon can be related to the residual crack opening observed at the unloading state, which induces tensile stresses in the area of the crack tip. These stresses interconnect the discontinuous micro-cracks. This mechanism, proposed by Horii et al (1992), may be the source of the crack growth under cyclic loading.

#### 3.2 Kinetic of crack growth

The projected crack lengths measured by taking successive replicas during a fatigue test, are presented versus the number of cycles " $n$ " in Fig. 5a, for all the tests. For high load levels, they are reported in Fig. 5b with a convenient scale for better clarity. It can be seen that the curves are

ordered with regard to the upper load level, except the one quoted (8\*). The case of this test will be discussed later.

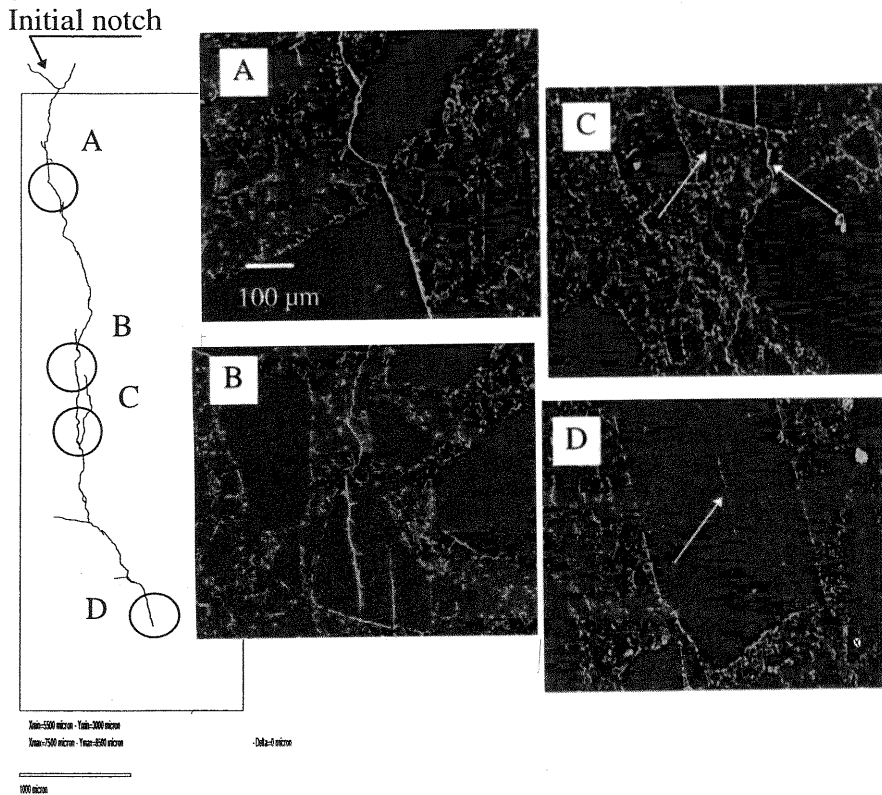


Fig. 4. Feature of the fatigue crack growth process.

(A) crack connecting with the interfacial zone, (B) Branching phenomenon within an aggregate, (C) Crack branching in the matrix, (D) Crack tip.

Generally, Paris's empirical model is used to describe the crack growth for many materials. It can be written as :

$$\frac{da}{dn} = C \left( \frac{\Delta K_I}{K_{IC}} \right)^m \quad (2)$$

$\Delta K$  is the variation of the amplitude of the stress intensity factor at the tip of the crack, assuming that linear elastic fracture mechanics apply.  $C$  and  $m$  are material constants.  $K_{IC}$  is the fracture toughness. The amplitude of

the stress intensity factor is calculated from linear elastic fracture mechanics, according to the Brown and Strawly's formula (1967) :

$$\Delta K_I = \frac{3\Delta Pl}{2bh^2} \sqrt{a} \Psi \left( \frac{a}{h} \right) \quad (3)$$

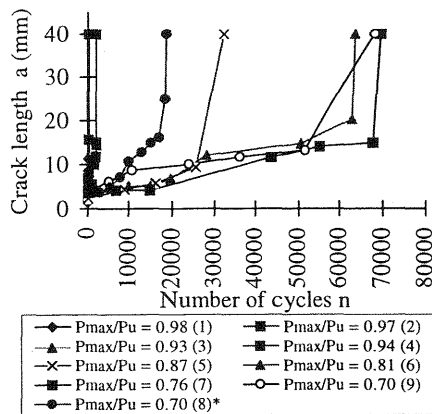


Fig. 5a. Crack length versus the number of cycles for all the tests

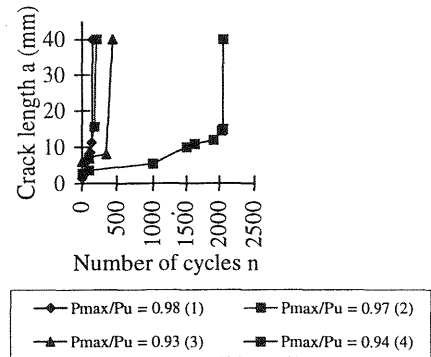


Fig. 5b. Crack length versus the number of cycles for high amplitude cycles

It is well known that at least in static tests, the stress free crack is extended by a non linear zone along which cohesive forces are transmitted (Karihaloo. 1995). This effect cannot be taken into account through equations (2) and (3).

By fitting the crack lengths versus the number of cycles by an exponential law, one can calculate the crack growth rate  $\frac{da}{dn}$ . Plotting this

rate versus the ratio  $\frac{\Delta K_I}{K_{IC}}$  in logarithmic coordinates, as shown in Fig. 6,

we can observe that the relation between  $\log \frac{da}{dn}$  and  $\log \frac{\Delta K_I}{K_{IC}}$  is linear. In addition the obtained values of coefficient  $m$  (table 2) are independent of the upper load level. Their mean value is approximately 3.

Taking the mean value of the exponent  $m$  gives the values of  $C$  reported in table 2. We can note that the coefficient  $C$  depends on the upper load level. This is illustrated in Fig. 7, in which we can observe that the parameter  $C$  is a function of the ratio  $P_{max}/P_u$ . Such a conclusion is in agreement with the work of Baluch et al (1987), where it is proposed that  $C$  could be a function of  $P_{min}/P_{max}$ . According to Fig. 7, two domains of

variation can be distinguished. For high load values a logarithmic correlation between  $P_{max}/P_u$  and  $C$  can be proposed as :

$$\frac{P_{max}}{P_u} = \alpha \ln C + \beta \quad \left( \frac{P_{max}}{P_u} \geq 0,85 \right) \quad (4)$$

For low load values,  $C$  appears to be approximately constant. In that case Paris's law would be valid at all.

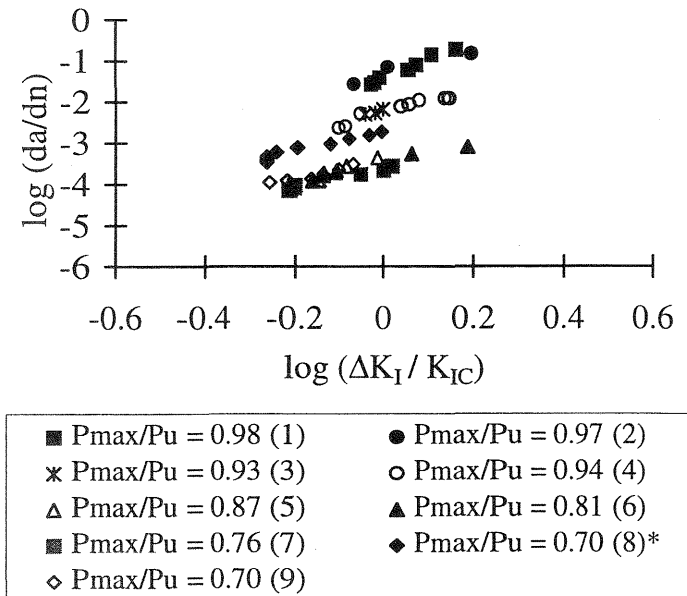


Fig. 6. Linear regression according to the Paris law

Table 2. Paris's parameters.

Test number	1	2	3	4	5	6	7	8*	9
$P_{max}/P_u$	0.98	0.97	0.94	0.93	0.87	0.81	0.76	0.70	0.70
Exponent $m$	2.64	4.54	2.76	2.85	4.18	2.31	2.25	2.60	2.38
Mean value $m$	2.94								
coefficient $C$ ( $m=2.94$ ) ( $\mu\text{m}/\text{cycle}$ )	45.7	48.9	5.50	6.40	0.38	0.33	0.26	2.06	0.45

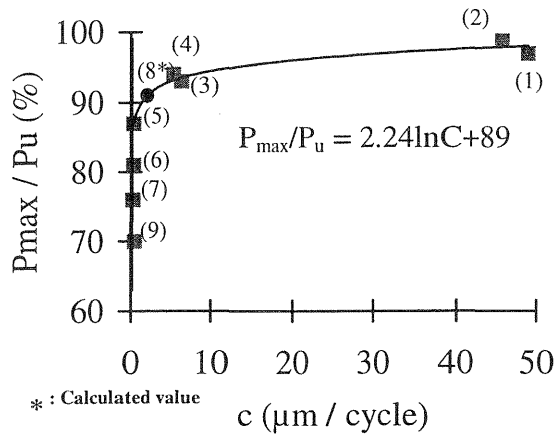


Fig. 7. Level of loading versus the parameter  $C$

Going back over Fig. 5a, a comment can be formulated about the curve quoted (8\*). Because it does not agree with the assumed arrangement of the curves, one can think that the actual strength of the specimen is lower than the mean value  $P_u$  determined in the static tests, and that the considered rate of loading is higher. According to the value of  $C$  in this test, Eq (4) would indicate that the level of loading is around  $0,91P_u$ , (marked by (8\*) in Fig. 7).

#### 4 Conclusions

- 1) Under fatigue tests, the measured crack length on the lateral surface can represent the length of the damage inside the specimen. In addition no discontinuous micro-cracks are observed inside the specimen in contrast to the static tests. This can be explained in part by the mechanism of crack growth under cyclic loading formulated by Horii et al.
- 2) The compliance calibration method underestimates the actual crack length. A linear regression between the relative crack length measured by replica method and compliance calibration is found.
- 3) The feature of crack growth is more complex than under static tests. More diffuse and branching phenomena are detected in both the matrix and the aggregates.
- 4) The parameter  $C$  of Paris's law, is a function of the upper load level. A logarithmic correlation can be used to link the upper load level to this parameter. For low load levels, Paris's law seems to be valid.

## References

- Bazant, Z. P. and Xu, K. (1991) Size effect in fatigue fracture of concrete. **ACI Materials Journal.**, 88 (4) 390-399.
- Bazant, Z. P. and Schell, W. F. (1993) Fatigue fracture of high strength concrete and size effect. **ACI Materials Journal.**, 90 (5) 472-478.
- Bascoul, A. Kharchi, F. and Maso, J.C. (1989) Concerning the measurement of the fracture energy of a micro-concrete according to the crack growth in a three points bending test on notched beams, in **Fracture of Concrete and Rock** (Eds. S.P. Shah and S.E. Swartz), Springer-Verlag, 396-408.
- Bascoul, A. and Turatsinze, A. (1994) Microstructural characterisation of mode I crack opening in mortar. **Materials and structures**, 27 (166) 71-78.
- Brown, W. E. and Strawly, J. E. (1967) Plain strain crack toughness testing of high strength metallic materials. **Special technical publication ASTM**, Philadelphia.
- Baluch, M. H., Quresh, A. B. and Azad, A. K. (1987) Fatigue crack propagation in plain concrete, in **Fracture of Concrete and Rock**, Proceedings of an International Conference, Houston, (Springer-Verlag, New York, 1989), 80-87.
- BAEL91. (1992) Règles techniques de conception et de calcul d'ouvrages en béton armé. Cahiers du CSTB.
- Hordijk, D. A. (1990) Local approach to fatigue of concrete. Technical thesis of university Delft.
- Horii, H., Shin, H. C. and Pallewatta, T. M. (1992) Mechanism of fatigue crack growth in concrete. **Cement and concrete composites**, 14 (2) 83-89.
- Hsu, T. T. C. (1984) Fatigue and microcracking of concrete. **Materials and Structures.**, 17 (97) 51-54.
- Karihaloo, B. L. (1995) **Fracture Mechanics & Structural Concrete**. Longman Scientific & Technical, USA.
- Murdock and Kestler. (1984) Long term random dynamic loading of concrete structures, RILEM Report Committee 36 RDL, **Materials and Structures**, 17 (97) 1-29.
- Ollivier, J. P. (1985) A non destructive procedure to observe the microcracks of concrete by scanning electron microscopy. **Cement and Concrete Research**, 15 (6) 1055 - 1060.
- Swartz, S.E. and Go, C.G. (1984) Validity of compliance calibration to cracked concrete beams in bending. **Experi. Mech**, 24 129-134.